Vietnam Journal of Catalysis and Adsorption
Tạp chí xúc tác và hấp phụ Việt Nam

http://jca.edu.vn

Development of a worm-hole structured $CuZnO_2$/MSU photocatalyst for enhanced antibiotic degradation

Ngo Ha Son[1,*], Nguyen Thi Linh[2]

[1] *Hanoi University of Mining and Geology, 18 Vien street, Hanoi, VIETNAM*
[2] *AMCA Research Group, Hanoi University of Mining and Geology*
**Email: ngohason@humg.edu.vn*

ARTICLE INFO

Received: 18/06/2024
Accepted: 19/09/2024
Published: 30/09/2024

Keywords:
MSU; $CuZnO_2$-based photocatalyst; Ciprofloxacin; photodegradation; waste water treatment.

ABSTRACT

In this study, a $CuZnO_2$/MSU photocatalyst was developed using a simple method and common resources. Characterization through XRD, BET, EDX, TEM, and SEM techniques revealed its worm-hole structure and uniform $CuZnO_2$ distribution. The catalyst exhibited a reduced band gap of 2.4 eV and a substantial surface area of 307 m^2/g, facilitating 94% degradation of Ciprofloxacin (CIP) within 4 hours of light exposure. Further investigation into the photodegradation process showed that a minimal catalyst quantity (10mg) and H_2O_2 oxidant led to 95% CIP transformation from a 30 ppm concentration, surpassing typical wastewater levels. Optimal efficiency was achieved with a 50/50 Cu^{2+}/Zn^{2+} ratio, indicating a synergistic effect. These results underscore the $CuZnO_2$/MSU catalyst's potential for antibiotic remediation in water.

1. Introduction

The contamination of water bodies with antibiotics, particularly ciprofloxacin, is a pressing environmental issue that has garnered significant attention in recent years. Ciprofloxacin (CIP), often used in the medical industry for treating bacterial infections, poses a serious threat to aquatic life and human health due to its toxicity and non-biodegradable nature. Therefore, the need for effective ciprofloxacin removal methods is paramount [1,2].

Antibiotic removal methods include physical, chemical, and biological processes. Physical methods like adsorption and filtration are efficient but can generate secondary pollutants. Chemical methods are effective but may use hazardous chemicals. Biological methods are eco-friendly but can be slow and less effective for certain antibiotics [3–5]. The photocatalytic process, which uses light to activate a catalyst to degrade antibiotics, has shown promise due to its non-selectivity, potential for complete mineralization of antibiotics, and sustainability [6,7].

However, the efficiency of the photocatalytic process heavily depends on the performance of the photocatalyst. The photocatalyst must have a high surface area for dye adsorption, excellent light absorption capability, and good charge separation efficiency to prevent the recombination of generated electron-hole pairs [8,9].

In this regard, the use of a catalytic support for the photocatalyst can enhance its stability and reusability, while also improving its photocatalytic performance. MSU, a mesoporous silica, is an ideal photocatalyst support due to its high surface area, tunable pore size, and thermal stability. Its high surface area allows for increased photocatalyst loading, improving dye degradation efficiency. Its tunable pore size facilitates molecule diffusion, enhancing photocatalytic

https://doi.org/10.62239/jca.2024.054

performance. Its thermal stability prevents photocatalyst sintering at high temperatures, maintaining activity over time. Additionally, MSU improves photocatalyst separation and recovery, making the process more sustainable and cost-effective [10,11].

Among various materials studied as potential catalytic active phases, $CuZnO_2$ has emerged as a promising candidate. Its simple and cost-effective synthesis process makes it suitable for large-scale production. $CuZnO_2$ exhibits excellent photocatalytic performance, as evidenced by its effectiveness in degrading various antibiotics. Its tunable band gap allows for optimized light absorption, a crucial factor in photocatalysis. Like ZnO, $CuZnO_2$ is chemically stable, ensuring the durability of $CuZnO_2$-based photocatalysts. Additionally, $CuZnO_2$'s ability to generate free electrons and holes when exposed to light enhances its photocatalytic reactions [12,13].

In light of these considerations, this paper aims to delve deeper into the research on CIP removal, with a particular focus on the photocatalytic process and the use of $CuZnO_2$ as an active phase. This research could contribute to the development of more efficient, sustainable, and eco-friendly solutions for antibiotics removal.

2. Experimental

Chemicals

The research made use of various chemicals including MSU (home-grown), distilled water, zinc diacetate 99% (Xilong, China), copper (II) nitrate trihydrate $Cu(NO_3)_2.3H_2O$ 99% (Xilong, China), Ciprofloxacin (CIP) with a purity of 99.99% (Merck, Germany), hydroperoxide 30% (Duc Giang Chemical Group, Vietnam), and Sodium hydroxide with a purity greater than 99% (Guangdong Guanghua, China). Every substance employed in the process was of the highest analytical quality and was utilized in its original form, with no further refinement necessary. The equipment used in the study comprised an analytical balance, a stirrer, 20W LED lamps, a drying oven, a muffle furnace, a one-neck flask, a reflux condenser, a glass rod, a graduated cylinder, and a pipette.

Synthesis of $CuZnO_2$/MSU

In the process of synthesizing a photocatalyst, zinc salt and NaOH were first dissolved in deionized water to form a precipitate solution. Copper salt and MSU support were then added to this mixture and stirred for 4-6 hours before being left to stand for 6-12 hours. The mixture was rinsed multiple times with deionized water to remove soluble CH_3COONa salt. It was then dried at 80°C for 6 hours to convert the copper salt to anhydrous $Cu(NO_3)_2$. Finally, the mixture was calcined at 400°C for 4 hours, causing the thermal decomposition of zinc hydroxide to form ZnO and copper salt to form CuO. These oxides adhered to the support, completing the synthesis process. The ratio of Cu^{2+}/Zn^{2+} was set at 50/50 and 30/70, the percentage of active phase is 70%, the weight of support is 0.5 g.

Material characterizations

X-ray diffraction (XRD) patterns were captured using a D8 Bruker device with Cu Kα radiation of wavelength 1.5403, scanning a range of 2θ = 5–80°. Energy-dispersive X-ray spectroscopy (EDX) data was collected using ESEM-XL30. The material's surface morphology was studied using Scanning electron microscopy (SEM), with images taken using a JSM-6701F (JEOL) instrument. A small amount of the suspension was placed on a silicon wafer for SEM sampling. Transmission electron microscopy (TEM) images were taken with a JEM2100 device (JEOL, Tokyo, Japan). The material's band gap energy and the amount of pollutants removed post-photocatalytic degradation were determined by recording UV-VIS spectra within a wavelength range of 200 to 800 nm, using a Jasco V-750. The Brunauer–Emmett–Teller (BET) nitrogen adsorption–desorption isotherm was performed at 77.34 °C using a CHEMBET-3030, allowing for the calculation of the material's specific surface area and pore size distribution. The point of zero charge was ascertained through the application of the drift technique, as documented in reference [14].

Photocatalytic activity evaluation

A 30 ppm CIP solution is prepared in a 50 ml volume and mixed with a known weight of catalyst. After an initial 30-minute adsorption, 0.25 ml of H_2O_2 is added and UV light activated. Hourly samples are collected for up to 4 hours. The conversion of CIP is computed using the formula:

$$\text{Conversion (\%)} = (C_o - C_t)/C_o \times 100\%$$

where C_o represents the initial concentration of CIP at t = 0 (hour), and C_t is the concentration of CIP in the solution post-reaction at time t. Concentrations are determined using UV-vis spectroscopy, specifically the 273 nm wavelength peak.

3. Results and discussion

XRD and BET results

https://doi.org/10.62239/jca.2024.054

The X-ray diffraction results of the $CuZnO_2$/MSU material are presented in Figure 1A, with a diffraction angle 2θ ranging from 2-80°. The X-ray spectrum of the $CuZnO_2$/MSU material shows peaks at 2θ angles of 31.9°, 34.5°, 36.3°, 47.7°, 56.7°, characteristic of the crystal reflection planes of ZnO [15], and peaks at 2θ angles of 32.6°, 35.6°, 38.8°, 48.8°, 53.6°, 58.3°, characteristic of the reflection planes of CuO [16]. Thus, the XRD measurement results have confirmed the presence of CuO and ZnO coated on the surface of the support.

It can be observed that when Cu^{2+} is doped, the diffraction peaks shift towards smaller 2θ angles compared to the diffraction peaks of ZnO. This shift is evident in the sample with a large amount of doped Cu^{2+} (Cu^{2+}/Zn^{2+} ratio is 50/50). This result is consistent with some previous results . The authors suggest that Zn^{2+} ions have been replaced by Cu^{2+} ions during the sample synthesis process. With a Cu^{2+}/Zn^{2+} ratio of 30/70, the peaks at 2θ angles of 35.6°, 38.8°, characteristic of the reflection planes of CuO, are not high, but with a ratio of 50/50, we see that the peak of CuO is high and clear. This indicates that Cu^{2+} ions have replaced the positions of Zn^{2+} ions. Thus, the XRD measurement results have confirmed the presence of CuO and ZnO coated on the surface of the support.

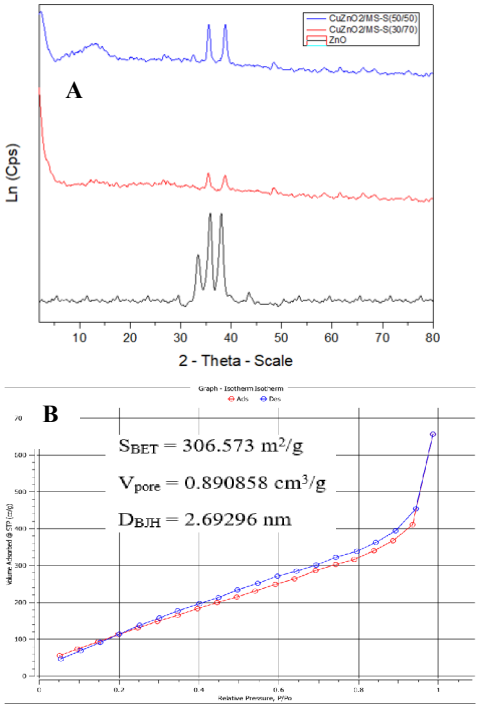

Figure 1: XRD spectrum (A) and N_2 isothermal adsorption-desorption curve (B) of $CuZnO_2$/MSU

To determine the specific surface area, pore volume, and pore diameter of $CuZnO_2$/MSU-S, the isothermal nitrogen adsorption method at 77.3K was conducted. The results are shown in Figure 1B.

The $CuZnO_2$/MSU-S photocatalyst, with a surface area of 307 m^2/g and a pore diameter of 2.7 nm, exhibits a type IV isothermal adsorption-desorption curve. It's effective for treating organic pollutants via adsorption-catalysis.

TEM and SEM results

The surface morphology of the material is characterized by the Transmission Electron Microscopy (TEM) and Scanning Electron Microscopy (SEM) methods. The results are presented in Figure 2.

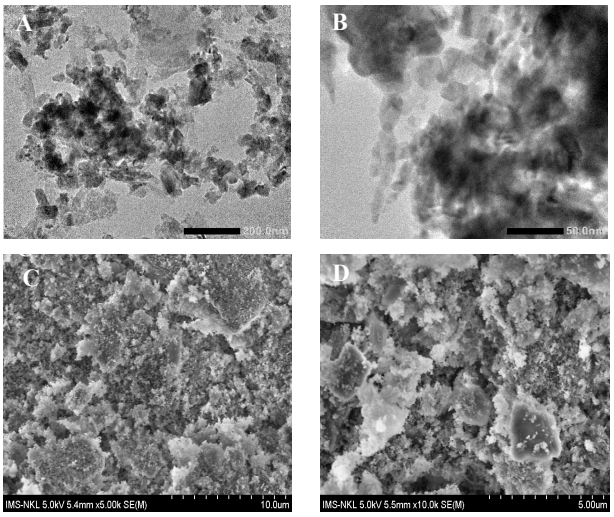

Figure 2: TEM (A, B) and SEM (C, D) images of $CuZnO_2$/MSU

The TEM images reveal small, uniform $CuZnO_2$/MSU photocatalyst particles, enhancing active sites for reactions. Particle aggregation may improve photocatalytic activity, and the rough surface texture could increase light absorption and reaction sites. Furthermore, contrast variations within the particles suggest a possible composite material or core-shell structure, with different components playing various roles in the photocatalytic process, such as light absorption, charge separation, or providing reaction sites.

SEM, as shown in Figure 2C and 2D, were taken at levels of 2 µm and 10 µm. The Scanning Electron Microscopy (SEM) results show the distribution of particles adhering to the surface of the support and are fairly evenly distributed. The addition of $CuZnO_2$ to the MSU support shows a significant effect in improving the surface of the catalyst.

https://doi.org/10.62239/jca.2024.054

Energy bandgap and elemental composition of the material

The bandgap energy of the catalyst material is determined using the UV-Vis diffuse reflectance spectroscopy method, and the results are shown in the figure 3.

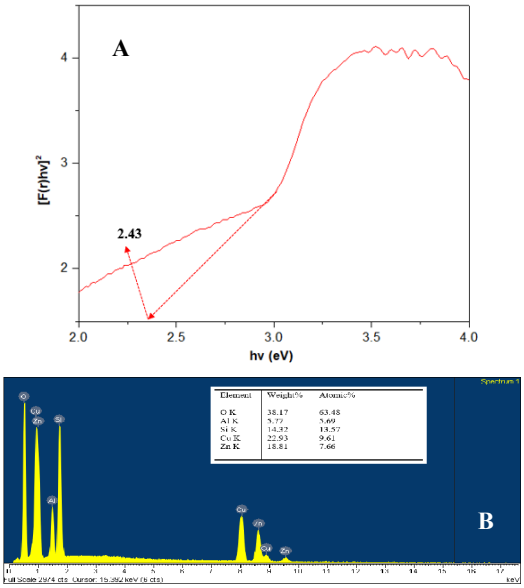

Figure 3: Bandgap energy (A) and EDX result (B) of $CuZnO_2$/MSU

From the results in Figure 3A, we can see that the bandgap energy (Eg) of the $CuZnO_2$/MSU material is 2.43 eV. This value indicates that the doping of Cu^{2+} reduces the bandgap energy of ZnO (3.37 eV). The EDX results (Figure 3B) of this material reveals the presence of silica oxide, copper oxide, zinc oxide, and aluminum oxide as the main components in the $CuZnO_2$/MSU-S material. The measurement results confirm that the main components are SiO_2, CuO, and ZnO. It is observed that the percentage composition of the catalyst components, Cu and Zn, are respectively 22 and 19%, which is fairly similar to the calculated Cu^{2+}/Zn^{2+} ratio of 50/50 during the synthesis of the sample.

Photocatalytic activity evaluation

The effect of solution's pH and contaminant concentration

To examine the effects of pH conditions and the initial concentration of ciprofloxacin (CIP) on its degradation, a series of experiments were performed wherein the pH value and CIP concentration were systematically varied. All other experimental conditions were held constant to ensure the validity of the results.

As can be seen, the $CuZnO_2$/MSU-S photocatalyst's degradation efficiency of CIP (20ppm) varies with pH: 74% at pH=4 and 94% at pH=7, but decreases to 91% at pH=10. This is due to electrostatic forces affecting the degradation rate. The catalyst has a point of zero charge (pH_{pzc}) of 9.2 (which was identified by Drift method [17]). Ciprofloxacin (CIP) exhibits amphoteric properties due to its molecular structure, which includes a carboxylic acid group with a pKa_1 of 5.76 and an amino group with a pKa_2 of 8.68. Its ionic state changes with the pH: below 5.76, it's predominantly cationic (CIP^+); above 8.68, it's anionic (CIP^-); and between these values, it exists mainly as a zwitterion ($CIP^\pm$). At pH=7.4, CIP is neutral, corresponding to its isoelectric point. Optimal performance is around pH=7 – 9, suitable for treating hard-to-degrade organic compounds like CIP. At this range, pH value of 4 is less ideal due to environmental concerns. The optimal pH range for CIP degradation is in accordance with previous work [18].

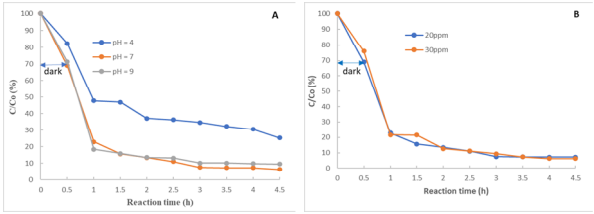

Figure 4: Effect of solution's pH (A) and CIP initial concentration (B) on CIP photodegradation efficiency

From the Figure 4B, it is observed that the transformation rate of CIP after 4 hours under UV stands at 94% (at 30 mg/L), nearly matching the transformation rate of 95% for CIP after 4 hours (at 20 mg/L). Consequently, it can be concluded that the transformation is nearly complete after 4 hours. Hence, it is evident that the catalyst possesses a high degradation efficiency for CIP, even at concentrations significantly exceeding those typically encountered in actual conditions [19], [20].

Effect of H_2O_2 dosage and ratio of Cu^{2+}/Zn^{2+} active phase

To explore the influence of Cu^{2+}/Zn^{2+} ratio on the degradation efficiency of ciprofloxacin (CIP), variations were made to the H_2O_2 content and the active phase ratio in the experiments. The outcomes obtained are depicted in Figure 5.

It was observed in Figure 5 that after four hours of illumination, the transformation rates of the samples with Cu^{2+}/Zn^{2+} ratios of 30/70 and 50/50 were 70% and 93%, respectively. This indicates that the sample synthesized with a Cu^{2+}/Zn^{2+} ratio of 50/50 exhibited superior performance compared to the 30/70 ratio.

The limitation of ZnO is the rapid recombination of electrons and photogenerated holes, which diminishes the photocatalytic effect. Therefore, doping Cu^{2+} ions

https://doi.org/10.62239/jca.2024.054

into Zn/MSU-S is necessary, with Cu^{2+} serving as electron traps to inhibit the recombination process, thereby extending the lifetime of the photogenerated holes to generate •OH radicals. Consequently, increasing the Cu^{2+}/Zn^{2+} ratio from 30/70 to 50/50 enhances the degradation efficiency of CIP by preventing the electron-hole recombination.

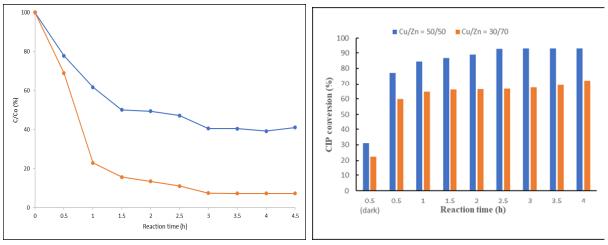

Figure 5: Effect of Cu^{2+}/Zn^{2+} ratio on CIP photodegradation efficiency

The photocatalytic efficacy largely depends on the separation of electron-hole pairs. Doping an n-type semiconductor onto a p-type semiconductor creates a p-n junction interface. Upon light excitation, the p-n material forms electron-hole pairs. Due to electrostatic interactions, the holes move towards the negative pole, while the electrons move towards the positive pole, promoting the separation of electron-hole pairs and enhancing photocatalytic efficiency.

Theoretically, the catalytic ability of semiconductors arises from the generation of electron-hole pairs upon light excitation; the e-/h+ pairs oxidize/reduce water to produce free radicals, which have the capability to photodegrade organic substances in aqueous solutions [21]. The photocatalytic activity of ZnO – CuO in the visible region is due to the presence of CuO. The bandgap of CuO is approximately 1.2 eV, while that of ZnO is about 3.37 eV. The intermixing of the conduction and valence bands of CuO and ZnO facilitates the electronic and hole transitions between the two semiconductors thermodynamically, narrowing the bandgap energy of the ZnO – CuO nanocomposite. Moreover, the separation of electron-hole pairs in the ZnO – CuO semiconductor prevents the recombination of e-/h+ pairs; when excited by visible light photons, the valence electrons of ZnO can generate electrons and holes, with the excited electrons moving to the conduction band (CB) of ZnO and the holes moving to the valence band (VB) of CuO. [17] The holes retained in the VB of CuO interact with H_2O to produce HO• free radicals. The electrons retained in the CB of ZnO interact with O_2, H_2O to produce $•O_2^-$ free radicals [21,22]. The photocatalytic oxidation reactions that degrade the antibiotic CIP occur via a similar mechanism [22,23] as follows:

$$p - CuO/n - ZnO + h\nu \rightarrow h^+ (CuO) + e^- (ZnO) \quad (1)$$

Upon the interaction of p-type CuO and n-type ZnO with photons (hν), the following photocatalytic reaction occurs:

$$h^+_{VB} + H_2O \rightarrow HO• + H^+ \quad (2)$$

$$e_{CB}^- + O_2 \rightarrow •O_2^- \quad (3)$$

$$2•O_2^- + 2H_2O \rightarrow H_2O_2 + 2HO^- + O_2 \quad (4)$$

$$H_2O_2 + e_{CB}- \rightarrow HO• + HO^- \quad (5)$$

$$h_{VB}^+ + HO^- \rightarrow HO• \quad (6)$$

These free radicals decompose organic compounds (for example, the antibiotic CIP):

$$HO• + CIP \rightarrow CO_2 + H_2O \quad (7)$$

Therefore, increasing the Cu^{2+}/Zn^{2+} ratio from 30/70 to 50/50 enhances the degradation efficiency of CIP by improving the inhibition of electron-hole recombination.

Effect of light intensity

Researching the impact of light intensity on photocatalytic degradation is crucial as it directly affects the efficiency of contaminant breakdown. The intensity and exposure duration to light are key factors that determine the effectiveness of the photocatalytic process by influencing electron excitation and the overall reaction kinetics. The results of light intensity effect on CIP degradation are introduced in Figure 6.

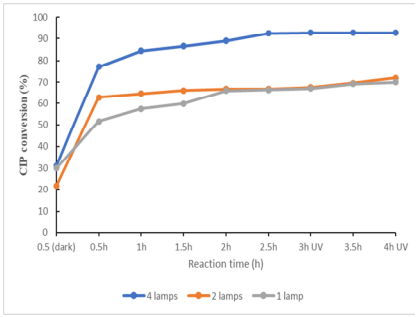

Figure 6. Effect of light intensity on CIP degradation

Based on the graph, it is observed that the conversion rate of CIP after 4 hours of UV exposure is 93% with four UV lamps, which is significantly higher compared to 71% and 69% with two and one lamp(s), respectively. At 4 hours of UV exposure, the conversion rate of CIP is 95% with four lamps, exceeding the rates with one and two lamps, which are 69% and 71%, respectively. This can be explained by the fact that increasing the intensity of illumination enhances the number of photons supplied to the reaction system, or equivalently, the energy provided for exciting electrons from the valence to the conduction band also increases [10]. This facilitates the photogenerated electron-hole pair separation process, leading to the

formation of a greater number of free radicals, thereby enhancing the photocatalytic activity of the material. As the light intensity increases, the number of photons entering the solution also rises, meaning that higher lamp intensity allows more photons to penetrate deeper into the solution layer and interact with more catalytic sites, which intensifies the process of generating free radicals such as •OH, thus increasing the photocatalytic activity of the material for the degradation of CIP [24,25].

When the photon quantity exceeds the oxidizing agent H_2O_2, it accelerates the formation of free radicals such as •OH and •OOH [26]. These radicals act as agents that decompose CIP through the mechanism:

$$H_2O_2 + \bullet OH \rightarrow \bullet HO_2 + H_2O \quad (8)$$

$$\bullet HO_2 + \bullet OH \rightarrow O_2 + H_2O \quad (9)$$

$$\bullet OH + CIP \rightarrow \text{products} \quad (10)$$

4. Conclusion

This investigation delved into the distinctive attributes of $CuZnO_2$/MSU catalysts. Analytical techniques such as XRD, BET, EDX, TEM, and SEM revealed that the catalyst boasts a substantial specific surface area of 307 m^2/g and a mesopore dimension around 3 nm. The material's low bandgap energy of roughly 2.4 eV contributes to its superior performance in photocatalytic processes. Remarkably, the catalyst achieved complete conversion of the antibiotic CIP at 20 ppm within 4 hours of exposure. The material point of zero charge was experimentally found to be 9.2. The study's pH trials at 4, 7, and 10 suggest that optimal photodegradation occurs between pH 6 to 9, at room temperature and standard atmospheric conditions. Furthermore, the dopant phase's influence, with Cu^{2+}/Zn^{2+} ratios of 30/70 and 50/50, was assessed, revealing that a 50/50 ratio leads to the peak degradation efficiency of 94% for CIP. These results could attribute to the advancement of photocatalytic technology for environmental cleanup and offers a promising solution for the sustainable management of water resources.

References

1. A.V. Samrot, S. Wilson, R.S. Sanjay Preeth, P. Prakash, M. Sathiyasree, S. Saigeetha, N. Shobana, S. Pachiyappan, V.V. Rajesh, Sustainability 15 (2023) 12639. https://doi.org/10.3390/su151612639
2. Fick, H. Söderström, R.H. Lindberg, C. Phan, M. Tysklind, D.G.J. Larsson, Environmental Toxicology and Chemistry 28 (2009) 2522–2527. https://doi.org/10.1897/09-073.1
3. O. Alegbeleye, O.B. Daramola, A.T. Adetunji, O.T. Ore, Y.J. Ayantunji, R.K. Omole, D. Ajagbe, S.O. Adekoya, Environ Sci Pollut Res 29 (2022) 56948–57020. https://doi.org/10.1007/s11356-022-21252-4
4. C.X. Chen, A. Aris, E.L. Yong, Z.Z. Noor, Environ Sci Pollut Res 29 (2022) 4787–4802. https://doi.org/10.1007/s11356-021-17365-x
5. U. Sen, B. Esteves, T. Aguiar, H. Pereira, Applied Sciences 13 (2023) 11963. https://doi.org/10.3390/app132111963.
6. X. Bai, W. Chen, B. Wang, T. Sun, B. Wu, Y. Wang, International Journal of Molecular Sciences 23 (2022) 8130. https://doi.org/10.3390/ijms23158130
7. N. Maldonado-Carmona, G. Piccirillo, J. Godard, K. Heuzé, E. Genin, N. Villandier, M.J.F. Calvete, S. Leroy-Lhez, Photochem Photobiol Sci 23 (2024) 587–627. https://doi.org/10.1007/s43630-024-00536-3
8. S. San Martín, M.J. Rivero, I. Ortiz, Catalysts 10 (2020) 901. https://doi.org/10.3390/catal10080901
9. M.A. Hassaan, M.A. El-Nemr, M.R. Elkatory, S. Ragab, V.-C. Niculescu, A. El Nemr, Top Curr Chem (Z) 381 (2023) 31. https://doi.org/10.1007/s41061-023-00444-7
10. 10. M. Náfrádi, G. Veréb, D.S. Firak, T. Alapi, Green Photocatalytic Semiconductors: Recent Advances and Applications, Springer International Publishing, Cham, 2022: 3–31. https://doi.org/10.1007/978-3-030-77371-7_1
11. S. Ullah, E.P. Ferreira-Neto, A.A. Khan, I.P.M. Medeiros, H. Wender, Photochem Photobiol Sci 22 (2023) 219–240. https://doi.org/10.1007/s43630-022-00299-9
12. A.B. Migdadi, M.K. Alqadi, F.Y. Alzoubi, H.M. Al-Khateeb, W.T. Bani-Hani, J Mater Sci: Mater Electron 33 (2022) 26744–26763. https://doi.org/10.1007/s10854-022-09341-z
13. K. Thangavelu, G. Abimannan, R. Rajendran, P. Arumugam, Ionics (2024). https://doi.org/10.1007/s11581-024-05603-4
14. M. Nasiruddin Khan, A. Sarwar, Surf. Rev. Lett. 14 (2007) 461–469. https://doi.org/10.1142/S0218625X07009517.
15. W. Muhammad, N. Ullah, M. Haroon, B. Haider Abbasi, RSC Advances 9 (2019) 29541–29548. https://doi.org/10.1039/C9RA04424H
16. A. Roy, A. Majumdar, J Mater Sci: Mater Electron 32 (2021) 27823–27836. https://doi.org/10.1007/s10854-021-07165-x
17. Y. Dadban Shahamat, M. Sadeghi, A. Shahryari, N. Okhovat, F. Bahrami Asl, M.M. Baneshi, Desalination and Water Treatment 57 (2016) 20447–20456. https://doi.org/10.1080/19443994.2015.1115372
18. H.-S. Ngo, T.-L. Nguyen, N.-T. Tran, H.-C. Le, Water 15 (2023) 1569. https://doi.org/10.3390/w15081569
19. A.S. Mutia, T. Ariyanto, I. Prasetyo, Water Air Soil Pollut 233 (2022) 146. https://doi.org/10.1007/s11270-022-05618-5
20. N. Javid, Z. Honarmandrad, M. Malakootian, DWT 174 (2020) 178–185. https://doi.org/10.5004/dwt.2020.24855
21. T.T. Minh, N.T.T. Tu, T.T. Van Thi, L.T. Hoa, H.T. Long, N.H. Phong, T.L.M. Pham, D.Q. Khieu, Journal of

Nanomaterials 2019 (2019) 5198045. https://doi.org/10.1155/2019/5198045

22. S. Pal, S. Maiti, U.N. Maiti, K.K. Chattopadhyay, CrystEngComm 17 (2015) 1464–1476. https://doi.org/10.1039/C4CE02159B
23. R. Saravanan, S. Karthikeyan, V.K. Gupta, G. Sekaran, V. Narayanan, A. Stephen, Materials Science and Engineering: C 33 (2013) 91–98. https://doi.org/10.1016/j.msec.2012.08.011
24. A. Enesca, L. Isac, T Materials 13 (2020) 2494. https://doi.org/10.3390/ma13112494
25. M. Náfrádi, G. Veréb, D.S. Firak, T. Alapi, Green Photocatalytic Semiconductors: Recent Advances and Applications, Springer International Publishing, Cham, 2022: 3–31. https://doi.org/10.1007/978-3-030-77371-7_1
26. T. Hirakawa, K. Yawata, Y. Nosaka, Applied Catalysis A: General 325 (2007) 105–111. https://doi.org/10.1016/j.apcata.2007.03.015